Microfluid Nanofluid (2015) 19:963–972
DOI 10.1007/s10404-015-1625-x

Theoretical and experimental analysis of thermoelectric lab-on-a-chip ELISA

Gergana G. Nestorova[1] · Niel D. Crews[2] · Eric J. Guilbeau[1]

Received: 3 June 2015 / Accepted: 7 August 2015 / Published online: 26 August 2015

Abstract Thermoelectric ELISA is a novel method for performing immunoassays in a microfluidic device in which the concentration of the analyte is determined by detecting the heat of the enzymatic reaction between glucose oxidase conjugated to an IgG detection antibody and glucose using a thin-film antimony–bismuth thermopile. The heat transfer in the system is mathematically modeled and the resulting differential equations solved using fundamental numerical methods. The theoretical analysis predicts the output voltage change of a thin-film thermopile positioned adjacent to the reaction zone. The predicted thermopile temperature increase is 0.35 m °C, which occurs 80 s after the substrate reaches the reaction zone. This temperature increase corresponds to a 2.45 μV peak height of the thermopile response and is easily detectable with 8-digit voltammetry electronics. The ELISA method was demonstrated experimentally by antibody-mediated detection of 8-hydroxydeoxyguanosine (8OHdG), an important biomarker of oxidative stress, in mouse urine samples. Experimental results correlate well with results from the mathematical simulations. Additional mathematical simulations were performed to evaluate the effect of flow rate and injection sample volume on the thermopile response. Results indicated that increasing the flow rate and decreasing the substrate injection volume decreased the magnitude and the duration of the thermoelectric response, but also accelerate the time required for sample analysis. The optimization of the flow rate and substrate injection volume is discussed herein.

1 Introduction

Enzyme-linked immunosorbent assay (ELISA) is an analytical technique in which the concentration of antigen, antibody, or analyte is determined by enzymatic activity measurements. It is based on the application of enzymes as labels and subsequent detection of an enzymatic reaction using luminescent (Mirasoli et al. 2014), chemiluminescent (Heyries et al. 2008), absorbance (Zhou et al. 2012), and electrochemical detectors (Pinacho et al. 2014). ELISA technology is used for accurate quantification of the amount of antigens (Haque et al. 2012) and miRNA (Tran et al. 2014) in clinical samples as well as pesticides and chemicals in environmental samples (Bibi et al. 2014).

While conventional ELISA techniques that are based on absorbance and fluorescent detection of analytes in plate reader instruments are well established, the measurement time is long. Some microfluidic solutions, such as lateral flow strip methods (Posthuma-Trumpie et al. 2009), have proven to be faster; however, the increased measurement speed in those techniques comes at the sacrifice of sensitivity that for some applications can be undesirable. ELISA technology based on electrochemical detection of the enzymatic reaction offers superior sensitivity. The disadvantage of the electrochemical detection method is the complexity of the electrochemical immunosensor coupled with limited

✉ Eric J. Guilbeau
ericg@latech.edu

Gergana G. Nestorova
ggnestor@latech.edu

Niel D. Crews
ncrews@latech.edu

[1] Biomedical Engineering Department, Louisiana Tech University, Ruston, LA, USA

[2] Institute for Micromanufacturing, Louisiana Tech University, Ruston, LA, USA

options for enzymatic labels that can generate electroactive enzymatic products (Ricci et al. 2012). Thermoelectric sensing of the heat product of the enzymatic reaction between a substrate and an enzyme linked to a detection antibody eliminates the need for complex optical systems while offering good sensitivity and fast response time.

Thermopiles are used as sensors in thermoelectric detection systems for detection of biochemical reactions because they have high common-mode thermal noise rejection and are well suited for miniaturization (Tangutooru et al. 2012). Thermoelectric methods have been used successfully in the past to measure small amounts of heat released during enzymatic reaction due to the remarkable sensitivity and room-temperature stability of thin-film thermopiles when operated in laminar flow streams. Levels of glucose (Guilbeau et al. 1987a, b; Muehlbauer et al. 1990), urea, and penicillin (Bataillard et al. 1993; Xie and Danielsson 1996) were measured by detecting the heat of the enzymatic reaction using thermopiles. Exothermic heat for glucose oxidation in the presence of glucose has been previously measured using antimony–bismuth thermopiles. The exothermic heat that is generated is estimated to be -79 kJ mol^{-1}. Glucose was detected thermoelectrically in both water (Tangutooru et al. 2012) and blood flowing under laminar flow conditions (Guilbeau et al. 1987a, b). The chemical reaction for oxidation of glucose in the presence of glucose oxidase is:

$$\text{Glucose} + O_2 + H_2O \xrightarrow{\text{Glucose Oxidase}} \text{Gluconic Acid} + H_2O_2 + 79\,\text{kJ mol} \quad (1)$$

Microfluidic calorimeters with integrated thermopiles detect the exothermic heat released during a chemical reaction and can be used to characterize a variety of chemical processes that do not require labeling of the analyte. Microfluidic calorimeters have the advantages of fast response and low application cost, combined with the capability of analyzing a small quantity of sample. They also provide the opportunity for portability and possible parallel processing. Calorimetry is an excellent tool for analysis of a broad spectrum of biochemical reactions. The output of the calorimeter depends on the flow rate, the concentration of the reactants as well as where the reaction occurs with respect to the hot junction of the thermopile (Zhang and Tadigadapa 2004). Measurement of small temperature changes using thermopiles requires control of the thermopile reference junction temperature to accurately differentiate the thermal signals from the noise (Lerchner et al. 2006).

Mathematical models of calorimeters with integrated thermopiles have proven to be helpful in specifying important parameters for optimal sensor design and performance. The effect of flow rates on the thermopile output of thermoelectric biosensor for glucose monitoring was mathematically modeled (Wang and Lin 2005). Results indicated that increasing the flow rates increases the heat loss via convective heat transfer and forced convection and as a result decreases the magnitude of the thermopile response. The effects of oxygen concentration, enzyme concentration, and flow rates on the thermoelectric signal for a glucose sensor were mathematically and experimentally analyzed (Muehlbauer et al. 1989). The magnitude of the thermopile output was proportional to the concentration of oxygen and enzyme and was inversely correlated with the velocity of the flow. Finite element methods have been used to optimize the thickness of the channel wall, length of reaction zone, and insulation to increase the signal for a thermoelectric enzyme sensor (Yiqun et al. 1995).

In this paper, we present an unsteady-state mathematical model that describes the temperature distribution and thermopile response in a microfluidic system for performing thermoelectric ELISA. In thermoelectric ELISA, the concentration of the analyte is determined by measuring the heat of the enzymatic reaction between a substrate and enzyme-linked reporter antibody using a thin-film thermopile. It is a new, rapid, easy-to-use, and inexpensive method for detection and quantification levels of analytes in biological and environmental matrixes. Lab-on-a-chip thermoelectric ELISA decreases the cost of the reagents and increases the potential for miniaturization and parallel processing by connecting multiple thermopiles. Multiple biological samples can be analyzed simultaneously by incorporating the array of thermopiles with a replaceable support for immobilization of the antigen or analyte. Additionally, the thermoelectric ELISA offers versatility in selecting the enzymatic label since the principle of operation is based on detecting the heat of the reaction.

Mathematical simulation of the thermopile response correlates with experimental results obtained by detecting 8-hydroxydeoxyguanosine (8OHdG) in mouse urine sample. 8OHdG is a biomarker of generalized oxidative stress and is linked to a number of aging-associated degenerative diseases such as cancer, diabetes, and atherosclerosis (Wu et al. 2004). In prior experimental study of thermoelectric ELISA, levels of 8OHdG were measured by binding to a monoclonal anti-8OHdG antibody that is immobilized to the surface of the lower channel wall of the microfluidic device and subsequent detection using glucose oxidase-conjugated secondary antibody. Glucose was introduced in the microfluidic system, and the heat of the enzymatic reaction was detected using thin-film antimony–bismuth thermopiles (Nestorova et al. 2015). While in the previous experimental work, the thermopile reference junctions were not under temperature control, the experimental result presented in this manuscript is obtained using Sb/Bi thin-film thermopile sensor that had reference junctions in contact with an aluminum heat sink. This experimental setup does

not allow heat dissipation from the measuring junctions to the reference junctions of the sensor and is relevant to the heat transfer mathematical simulations presented in this work.

1.1 Overview of thermoelectric lab-on-a-chip method for performing ELISA

The thermoelectric method for performing ELISA analyzed in this paper measures the heat generated in reaction (1). The analyte is bound to a capture antibody, and the concentration of the analyte is determined using enzyme labeled detection antibody. The primary antibody is immobilized to the microfluidic device channel wall to form a capture antibody/analyte/detection antibody complex. This complex is then exposed to a laminar flow stream of liquid to which the substrate for the enzymatic reaction is added. The heat released during the enzymatic reaction increases the temperature of the analyte/antibody complex, causing a transfer of heat from the complex to the fluid flowing in a laminar flow over the complex and toward the thermopile sensor. The temperature of the lower channel wall, under the reaction zone, increases when glucose is oxidized. The temperature change is detected by the measuring junctions of the thermopile, but not by the reference junctions. The change in the thermopile emf resulting from the increased temperature difference is measured with a nanovoltmeter. The magnitude of the thermoelectric signal is related to the concentration of the captured analyte.

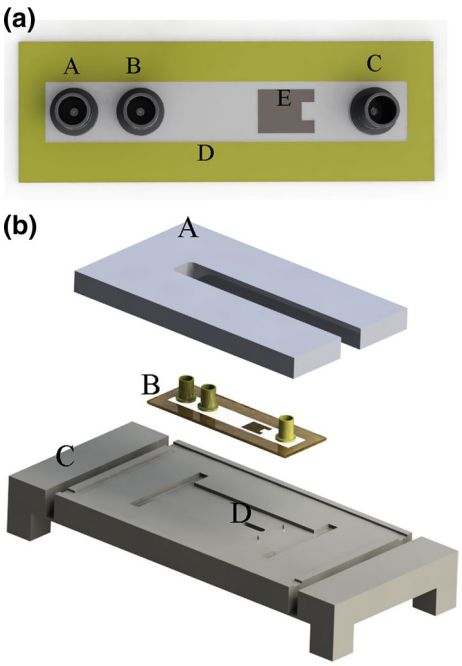

Fig. 1 **a** Schematic of microfluidic device with integrated thin-film thermopile. *A* is inlet 1 that supplies the buffer solution that hydrodynamically constrains the glucose solution, *B* is inlet 2 that supplies glucose, *C* is outlet/waste, *D* is Kapton tape that forms the channel wall, and E is the thermopile. **b** Exploded view of microfluidic device and aluminum holder. *A* is the *top* of the holder, *B* is the microfluidic device, *C* is the *bottom* part of the holder, and *D* is the air gap. The reference junctions of the thermopile are in contact with the aluminum block that serves as a heat sink and maintains constant temperature. The area of the reaction zone is located above the measuring junctions of the thermopile which is positioned over the air gap

Thermoelectric detection of the enzymatic reaction between the glucose oxidase labeled detection antibody and glucose was performed in a microfluidic device (Fig. 1a). The microfluidic chip consisted of two inlets and a single outlet. The lower channel wall consisted of a 25 mm × 75 mm streptavidin-coated glass cover slip. The upper channel wall consisted of a 25 mm × 75 mm microscope glass slide. The thickness of the glass slide was 1 mm, and the thickness of the cover slip was 175 μm. The channel was fabricated using 100-μM-thick double-sided Kapton® tape. The measuring junctions of the thermopile were positioned over an aluminum heat sink, while the reference junctions were positioned over an air gap built in the aluminum holder. This experimental setup prevents the temperature of the reference junctions to increase due to the heat released during the enzymatic reaction (Fig. 1b). During operation, simultaneous laminar flow at inlet 1 and inlet 2 restricts the substrate mixture to the middle of the region of the flow channel, in the vicinity of the sensing thermopile junctions. The chemical reagents are transported in the microfluidic device via the motion of fluids. The motion of fluids inside the channel could be efficiently controlled by flow focusing. Hydrodynamic focusing of fluids is achieved when the sample flow from inlet 2 is constrained laterally within the center of the channel by the flow of inlet 1 channel. The width of the focused stream can be controlled by adjusting the relative flow rates of inlet 1 and inlet 2 (Lee et al. 2006). The integration of the microfluidic components with the fluid handling and the data acquisition system was described in previously published work (Nestorova et al. 2015).

2 Experimental section

2.1 Mathematical model

A mathematical model that simulates the heat transfer within the microfluidic device as a result of the enzymatic reaction between glucose conjugated to an IgG detection antibody and glucose oxidase was developed and solved using fundamental numerical methods. A side view schematic of the microfluidic device is shown in Fig. 2. The model predicts the output voltage change of a thin-film thermopile attached to the lower channel wall of the device. The model assumes that the mass flow rate and the physical properties of the materials and the solution are constant

and the system is well insulated. Other assumptions that are included in the model are homogeneous heat generation and negligible axial mass diffusion.

Energy balances were performed for the fluid flowing within the channel of the device, the channel wall adjacent to the respective reaction zone, and the thermopile support. The general form of the energy balance equation is:

> The rate of accumulation of thermal energy within the system = the net rate at which thermal energy enters the system as a result of bulk fluid flow + net rate at which thermal energy enters the system via conduction and/or convection + volumetric rate of thermal energy generation by the enzymatic reaction.

The temperature difference detected by the thermopile (polyimide temperature below the reaction zone–polyimide temperature below the rinse solution) depends on the geometry of the microfluidic device, the physical properties of the system, the rate of flow through the chip, and the concentration of the substrate and the enzyme. The resulting mathematical model consisted of five ordinary differential equations that predict the change in the temperature of the fluid above the reaction zone, the two walls of the microfluidic channel above and below the reaction zone, the polyimide thermopile support film which is in contact with the measuring and reference junctions of the thermopile, and the acrylic tape that protect the thermopile. The equations were solved using the Radau numerical integration method for stiff systems. The thermopile output as a function of time was calculated by multiplying the theoretical thermopile sensitivity and the predicted variation in wall temperature assuming a 60-junction antimony–bismuth thin-film thermopile with a theoretical sensitivity of 7.14 μV mK^{-1}. A summary of the simulation parameters is given in Table 1.

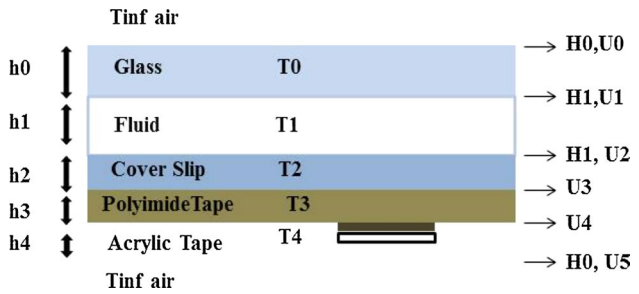

Fig. 2 Side view schematics of the microfluidic device. *Upper channel* wall is formed of glass slide; *lower channel* wall is formed of glass cover slip. The channel is filled with the buffer. Thin-film Sb/Bi thermopile is fabricated on polyimide support and attached to the outer surface of the lower channel wall using highly thermally conductive silver compound. The thermopile is protected with thin layer of acrylic tape. T1, T2, T3, T4, and T5: temperatures in the *middles* of each layer. H1, H2, H3, H4, and H5 and convection and conduction coefficient. U1, U2, U3, U4, and U5 are the overall heat transfer coefficients for each layer. h1, h2, h3, h4, and h5 are the thickness of each layer

The model assumes that the enzymatic reaction occurs at the inner surface of the lower channel wall, directly atop the measuring junctions of the thermopile. The upper channel wall of the microfluidic device is a 1.0-mm-thick glass microscope slide. The lower channel wall consists of a 175-μm-thick glass cover slip. The thermopile is fabricated on 125-micron-thick polyimide tape and is protected with acrylic tape. The hydraulic diameter of the channel was calculated using Eq. (2):

$$D_h = \frac{2wh_1}{w + h_1} \tag{2}$$

where h_1 is the height of the microfluidic device channel and w is the width of the reaction zone.

The thermal convection coefficient assuming the properties of pure water was calculated using Eq. (3):

$$H_1 = 7.54\frac{k_{\text{water}}}{D_h} \tag{3}$$

where the Nusselt number for fully developed laminar flow in a rectangular flow channel when the ratio of width to height of the channel is infinity is equal to 7.54. (Incropera 2011) The values for the overall heat transfer coefficients for each layer were calculated according to Eqs. (4), (5), (6), (7), (8), and (9).

$$U_0 = \frac{1}{\frac{1}{H_0} + \frac{\frac{h_0}{2}}{k_0}} \tag{4}$$

$$U_1 = \frac{1}{\frac{1}{H_1} + \frac{\frac{h_0}{2}}{k_0}} \tag{5}$$

$$U_2 = \frac{1}{\frac{1}{H_1} + \frac{\frac{h_2}{2}}{k_0}} \tag{6}$$

$$U_3 = \frac{1}{\frac{\frac{h_3}{2}}{k_2} + \frac{\frac{h_2}{2}}{k_0}} \tag{7}$$

$$U_4 = \frac{1}{\frac{\frac{h_3}{2}}{k_2} + \frac{\frac{h_4}{2}}{k_4}} \tag{8}$$

$$U_5 = \frac{1}{\frac{1}{H_0} + \frac{\frac{h_4}{2}}{k_4}} \tag{9}$$

The area where the enzymatic reaction occurs is labeled as A_s. The heat generated by the enzymatic reaction, labeled as

Table 1 Values of parameters used in the mathematical simulations

Symbols	Parameters	Values	Units
Glass slide	Glass		
ρ_0	Glass density	2.6	gm cm^{-3}
C_0	Glass heat capacity	0.2	cal gm^{-1} K^{-1}
K_0	Glass thermal conductivity	0.96	W m^{-1} K^{-1}
h_0	Glass slide thickness	1×10^{-3}	m
$T_0(0)$	Initial glass slide temperature	298	K
Fluid	Water		
ρ_3	Water density	1.0	gm cm^{-3}
C_3	Water heat capacity	1.0	cal gm^{-1} K^{-1}
K_3	Water thermal conductivity	0.58	W m^{-1} K^{-1}
T_{in}	Inlet water temperature	298	K
$T_1(0)$	Initial water temperature	298	K
H_1	Water convection coefficient	22,590	W m^{-2} K^{-1}
h_1	Channel height	1×10^{-6}	m
Glass coverslip	Glass		
ρ_0	Glass density	2.6	gm cm^{-3}
C_0	Glass heat capacity	0.2	cal gm^{-1} K^{-1}
K_0	Glass thermal conductivity	0.96	W m^{-1} K^{-1}
h_0	Glass coverslip thickness	175×10^{-6}	m
$T_2(0)$	Initial glass coverslip temperature	298	K
Thermopile	Polyimide tape		
ρ_2	Polyimide density	1.42	gm cm^{-3}
C_2	Polyimide heat capacity	0.26	cal gm^{-1} K^{-1}
K_2	Polyimide thermal conductivity	0.155	W m^{-1} K^{-1}
h_3	Polyimide thickness	125×10^{-6}	m
$T_3(0)$	Polyimide initial temperature	298	K
Protective tape	Acrylic tape		
ρ_4	Acrylic density	1.2	gm cm^{-3}
C_4	Acrylic heat capacity	0.35	cal gm^{-1} K^{-1}
K_4	Acrylic thermal conductivity	0.2	W m^{-1} K^{-1}
h_4	Acrylic thickness	109×10^{-6}	m
$T_4(0)$	Acrylic initial temperature	298	K
Air	Air		
ρ_1	Air density	1.29×10^{-3}	gm cm^{-3}
C_1	Air heat capacity	0.239	cal gm^{-1} K^{-1}
K_1	Air thermal conductivity	0.0227	W m^{-1} K^{-1}
H_0	Air convection coefficient	25	W m^{-2} K^{-1}
T_{inf}	Air temperature	298	K
Q	Flow rate	25	μL min^{-1}
A_s	Area of reaction zone	24×10^{-6}	mm^{-2}
Surf_heat	Power of reaction	1.22×10^{-6}	J s^{-1}
S_{coef}	Seebeck coefficient	7.2	μV mK^{-1}
J	Energy of the reaction	73.3×10^{-6}	J
Glass slide	Glass		
ρ_0	Glass density	2.6	gm cm^{-3}
C_0	Glass heat capacity	0.2	cal gm^{-1} K^{-1}
K_0	Glass thermal conductivity	0.96	W m^{-1} K^{-1}
h_0	Glass slide thickness	1×10^{-3}	m
$T_0(0)$	Initial glass slide temperature	298	K

Table 1 continued

Symbols	Parameters	Values	Units
Fluid	Water		
ρ_3	Water density	1.0	gm cm^{-3}
C_3	Water heat capacity	1.0	cal gm^{-1} K^{-1}
K_3	Water thermal conductivity	0.58	W m^{-1} K^{-1}
T_{in}	Inlet water temperature	298	K
$T_1(0)$	Initial water temperature	298	K
H_1	Water convection coefficient	22,590	W m^{-2} K^{-1}
h_1	Channel height	1×10^{-6}	m
Glass coverslip	Glass		
ρ_0	Glass density	2.6	gm cm^{-3}
C_0	Glass heat capacity	0.2	cal gm^{-1} K^{-1}
K_0	Glass thermal conductivity	0.96	W m^{-1} K^{-1}
h_0	Glass coverslip thickness	175×10^{-6}	m
$T_2(0)$	Initial glass coverslip temperature	298	K
Thermopile	Polyimide tape		
ρ_2	Polyimide density	1.42	gm cm^{-3}
C_2	Polyimide heat capacity	0.26	cal gm^{-1} K^{-1}
K_2	Polyimide thermal conductivity	0.155	W m^{-1} K^{-1}
h_3	Polyimide thickness	125×10^{-6}	m
$T_3(0)$	Polyimide initial temperature	298	K
Protective tape	Acrylic tape		
ρ_4	Acrylic density	1.2	gm cm^{-3}
C_4	Acrylic heat capacity	0.35	cal gm^{-1} K^{-1}
K_4	Acrylic thermal conductivity	0.2	W m^{-1} K^{-1}
h_4	Acrylic thickness	109×10^{-6}	m
$T_4(0)$	Acrylic initial temperature	298	K
Air	Air		
ρ_1	Air density	1.29×10^{-3}	gm cm^{-3}
C_1	Air heat capacity	0.239	cal gm^{-1} K^{-1}
K_1	Air thermal conductivity	0.0227	W m^{-1} K^{-1}
H_0	Air convection coefficient	25	W m^{-2} K^{-1}
T_{inf}	Air temperature	298	K
Q	Flow rate	25	μL min^{-1}
A_s	Area of reaction zone	24×10^{-6}	mm^{-2}
Surf_heat	Power of reaction	1.22×10^{-6}	J s^{-1}
S_{coef}	Seebeck coefficient	7.2	μV mK^{-1}
J	Energy of the reaction	73.3×10^{-6}	J

surf_heat, was calculated by considering the activity of glucose oxidase according to the vendor (Abcam, Cambridge, MA), moles of capture antibody, and analyte immobilized within the reaction zone. The rate of energy conversion per unit time is calculated according to the equation below:

$$\text{Surf\_heat} = \frac{J}{\text{sec}} \tag{10}$$

where J is the energy released during the enzymatic reaction. One unit of the enzyme oxidizes 1 μmol of glucose to gluconic acid per minute. Due to steric interactions of the surface immobilized antibodies, 928 fmols can be immobilized within the reaction zone, directly above the measuring junctions of the thermopile. The maximum concentration of 8OHdG captured within the area of the reaction zone is 928 fmols. It corresponds to 0.93×10^{-3} units of glucose oxidase immobilized over the reaction zone (Wiseman and Frank 2012). The concentration of the enzyme limits the amount of glucose that can be oxidized per unit time. Based on the specific activity of glucose oxidase, it is calculated that 930 pmols of glucose can be converted to gluconic acid per minute. Oxygen concentration during

the enzymatic reaction was 0.2 mM that corresponds to atmospheric levels of oxygen. The amount of heat that is generated by the enzymatic reaction for 8OHdG surface concentration of 928 fmols is 1.22 μJ s^{-1}. The duration of the enzymatic reaction is defined by the volume of the injection sample containing glucose and the flow rate.

Five differential equations were developed and solved using fundamental numerical method, Eqs. (11)–(15). For the mathematical simulations presented below, the heat source is included within the cover slip. While the reaction zone sits atop the coverslip, due to its small thickness, the model simulates it as part of the glass. Assigning a zone of its own will not lead to significant changes in the temperature distribution in the system.

Glass equation:

$$\rho_0 c_0 V_0 \left(\frac{\mathrm{d}}{\mathrm{d}t} T_0(t)\right) = U_1 A_s (T_1(t) - T_0(t)) - U_0 A_s (T_0(t) - T_{\mathrm{inf}}) \quad (11)$$

Fluid equation:

$$\rho_3 c_3 V_1 \left(\frac{\mathrm{d}}{\mathrm{d}t} T_1(t)\right) = U_2 A_s (T_2(t) - T_1(t)) + Q\rho_3 c_3 (T_{\mathrm{in}}(t) - T_1(t)) - U_1 A_s (T_1(t) - T_0(t)) \quad (12)$$

Cover slip equation:

$$\rho_0 c_0 V_2 \left(\frac{\mathrm{d}}{\mathrm{d}t} T_2(t)\right) = \mathrm{surf\_heat}(t) - U_2 A_s (T_2(t) - T_1(t)) - U_3 A_s (T_2(t) - T_3(t)) \quad (13)$$

Polyimide tape equation:

$$\rho_2 c_2 V_3 \left(\frac{\mathrm{d}}{\mathrm{d}t} T_3(t)\right) = U_3 A_s (T_2(t) - T_3(t)) - U_4 A_s (T_3(t) - T_4(t)) \quad (14)$$

Acrylic tape equation:

$$\rho_4 c_4 V_4 \left(\frac{\mathrm{d}}{\mathrm{d}t} T_4(t)\right) = U_4 A_s (T_3(t) - T_4(t)) - U_5 A_s (T_4(t) - T_{\mathrm{inf}}) \quad (15)$$

Simulations were performed using different flow rates and different volume of injected glucose (55 mM; Table 2).

2.2 Experimental methods

Materials and methods for the detection of 8OHdG are described in previously published work (Nestorova et al. 2015). Briefly, anti-8OHdG capture antibody conjugated to biotin was immobilized to the streptavidin-coated lower channel wall of the microfluidic device, in the area directly above the measuring junctions of the thermopile. The analyte, 8OHdG, was captured by the primary antibody and detected using secondary IgG antibody conjugated to glucose oxidase. A 50 mM citrate/phosphate buffer, pH 5.3, was introduced through inlet 1 of the microfluidic device. A 50 mM citrate/phosphate buffer, pH 5.3, buffer solution containing glucose was introduced through inlet 2 of the microfluidic chip. The glucose-containing solution was hydrodynamically focused over the reaction zone, and the heat of the enzymatic reaction between glucose and glucose oxidase was detected by the thermopile. The flow rates used for the experiment were 100 μL min^{-1} for inlet 1 and 25 μL min^{-1} for inlet 2. The size of the reaction zone was 3 mm × 6 mm, and the concentration of glucose was 55 mM. The volume of the injected glucose sample was 52 μL.

Table 2 Parameters used for mathematical simulations of heat transfer in the microfluidic system

Simulation number	Inlet 2 flow rate (μL min^{-1})	Glucose (55 mM) volume (μL)
1	25	52
2	25	26
3	12.5	52
4	12.5	26

While previously published work was done using thermopile sensor that are not under a temperature control, the experimental results presented in this manuscript were obtained using a microfluidic device with integrated Sb/Bi thin-film thermopile that had have reference junctions in contact with an aluminum heat sink to prevent heat dissipation toward the reference junctions of the thermopile.

3 Results and discussion

Mathematical simulations were performed using a flow rate of 25 μL min^{-1} through inlet 2 and a glucose sample volume of 52 μL. The model predicts a maximum surface heat of 1.22 μJ that produces a maximum thermopile thermoelectric emf change of 2.45 μV (Fig. 3a, b). The predicted thermopile signal duration is 250 s. The maximum thermopile output is reached 80 s from the initiation of the enzymatic reaction between glucose and glucose oxidase. The experimental value of the thermopile signal response obtained using the same parameter was 2.2 μV. The values of the predicted and the experimental values for the peak height of the signal are in close agreement and validate the accuracy of the mathematical model (Fig. 3b).

Reducing the sample injection volume from 52 to 26 μL and the flow rate from 25 to 12.5 μL min^{-1} decreased the

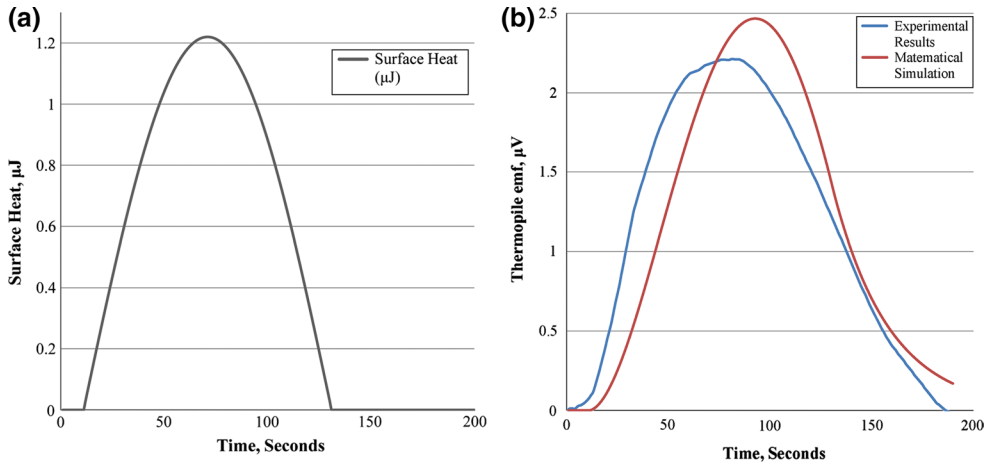

Fig. 3 **a** Mathematical simulation of surface heat change as a function of time. The flow rate of the substrate (glucose, 55 mM) is 25 μL min^{-1}, and the injection sample volume is 52 μL. **b** Mathematical simulation and experimental results for thermopile signal response. Substrate flow rate is 25 μL min^{-1}, and glucose (55 mM) injection volume is 52 μL. The temperature difference between the measuring and the reference junctions of the thermopile is recorded by a nanovoltmeter and processed using LabView software

total amount of heat that is generated by the reaction, the duration of the thermopile response, and the magnitude of the thermopile response peak height. The duration of the predicted thermopile response decreases from 250 to 190 s as the volume of introduced substrate is decreased from 52 to 26 μL, while the flow rate was maintained at 25 μL min^{-1}. Under the same experimental conditions, the peak height of the predicted thermopile response decreased from 2.45 to 1.9 μV (Fig. 4a). Decreasing the volume of injected glucose while maintaining flow rate of 12.5 μL min^{-1} reduces the peak of the thermopile signal from 3.8 to 3.1 μV and the duration of the thermoelectric response from 400 to 300 s (Fig. 4a). Reducing the volume of glucose decreases the duration of the reaction, and as a result less heat is detected by the thermoelectric sensor and can be dissipated faster. The rate of heat dissipation can be further increased by increasing the flow rate, but at the expense of signal strength.

Reducing the flow rate of inlet 2 from 25 to 12.5 μL min^{-1} while maintaining the same volume of glucose affected the magnitude and duration of the predicted thermopile signal. Simulations using a 26 μL glucose sample volume predicted that the magnitude of the thermopile signal will decrease from 3.1 to 1.9 μV as the flow rate is increased. The same trend was observed when the glucose volume was 52 μL. Under those experimental conditions, the signal increased from 2.45 to 3.8 μV as the flow rate decreased (Fig. 4a). Additionally, as the flow rate decreases, the temperature change of the polyimide thermopile support is reduced from 0.55 to 0.25 mK (Fig. 4b). The temperature of the fluid in the channel will increase from 0.35 to 0.55 mK as the velocity of the fluid is reduced (Fig. 4c). This is caused by a combination of two factors. Lower flow rate allows for longer time of diffusion of the substrate to the lower channel wall, and as a result more glucose molecules react with the enzyme. After the enzymatic reaction is completed, the temperature of the reaction zone starts to decrease. When the flow rate is reduced, the rate of heat efflux through the flow stream also decreased. This leads to lower rate of heat dissipation from the reaction zone and increase in the thermoelectric signal response.

The mathematical model assumes that there is no lateral heat transfer from the reaction zone toward the reference junctions of the thermopile. Because the reference junctions of the thermopile were positioned over a heat sink, the heat that dissipated toward the reference junctions of the thermopile was transferred toward the aluminum heat sink. As a result, the reference junctions are under constant temperature control (Fig. 1b). Since the output of the thermopile is a function of the difference between the measuring and reference junctions, maintaining the reference junctions over a heat sink increases the sensitivity of the sensor.

Oxygen concentration is an important factor that affects the efficiency of the enzymatic reaction. The number of glucose molecules that are converted to gluconic acid depends on the number of enzyme molecules that are immobilized within the area of the reaction zone and the activity of the enzyme. The enzymatic reaction converts 930 pmols of glucose to gluconic acid that consumes 930 pmols of oxygen per minute. For a flow rate of 25 μL min^{-1} and atmospheric oxygen levels, 5000 pmols of oxygen is introduced in the system per minute. According to these calculations, atmospheric levels of oxygen are not a limiting factor in our experiments. Oxygen concentration becomes a limiting reaction factor when the concentration of oxidized

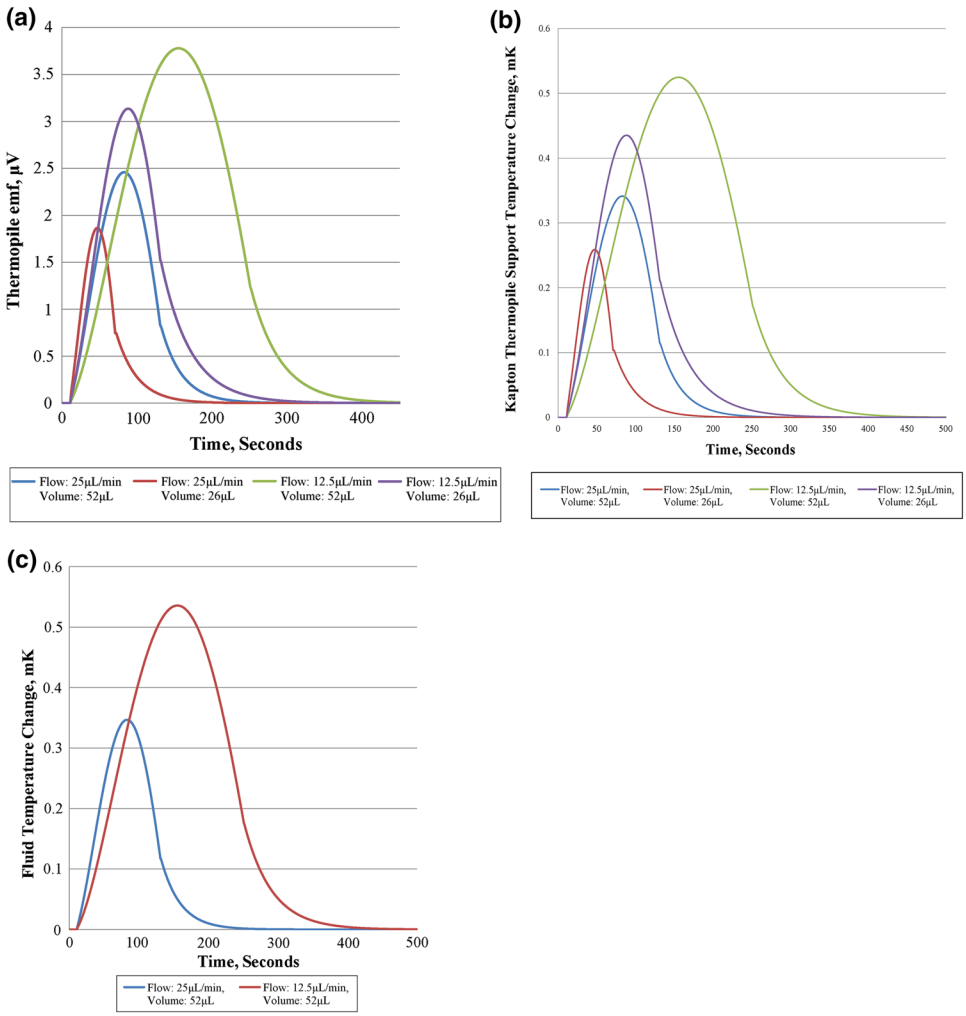

Fig. 4 **a** Mathematical simulation of the effect of fluid flow rate and injection substrate volume on the thermopile voltage output. Simulations were performed using flow rates of 25 and 12.5 μL min^{-1} for inlet 2 and glucose (55 mM) sample volume of 52 and 26 μL. **b** Mathematical simulations of the effect of flow rate and glucose injection volume on the temperature change between the measuring and reference junctions of the thermopile. **c** Mathematical simulations of the effect of flow rate on the temperature change (mK) of the fluid that fills the microfluidic channel. The temperature increase is due to the enzymatic reaction between glucose and glucose oxidase that occurs at the inner surface of the inner channel wall of the microfluidic device

glucose molecules per minute increases to more than 5 nmols. This is a function of reaction zone size, specific activity of enzyme, and concentration of glucose.

The optimal conditions for performing ELISA are a balance between signal strength that relates to sensitivity of detection and the duration of the signal. The mathematical simulations reveal that higher flow rate coupled with decreased sample injection volume decreased the time it requires for the signal response to reach maximum height while maintaining measurable signal response.

4 Conclusions

The mathematical model, described in this manuscript, is a valuable tool that can be used to maximize the signal output and optimize the parameters and design of the microfluidic device for performing thermoelectric ELISA. Experimental results correlate with the predicted values for the thermopile voltage output. Mathematical simulations confirm that the duration of the enzymatic reaction and the velocity of the fluid have significant effect on the thermopile response. Future work will include improving the design of the microfluidic device to reduce heat loss and increase sensitivity and magnitude of the signal. This will include selecting and testing of materials for fabrication of the upper channel that have lower thermal conductivity. Reducing the thermal conductivity and heat capacity of the material that forms the lower channel wall decreases the loss of heat toward the thermopile. In a second generation of the lab-on-a-chip device, the thermoelectric sensor will be deposited on the inside of the lower channel wall and protected by a thin layer of insulating material.

References

Bataillard P, Steffgen E, Haemmerli S, Manz A, Widmer HM (1993) An integrated silicon thermophile as biosensor for the thermal monitoring of glucose, urea and penicillin. Biosens Bioelectron 8:89–98

Bibi S, Ahmed W, Alam SE (2014) Comparison of rapid test with ELISA for the detection of hepatitis B surface antibodies. Pak J Med Res 53:60

Guilbeau EJ, Clark LC, Pizziconi VB, Schultz JS, Towe BC (1987a) Biosensors in artificial organs. ASAIO J 33:834–836

Guilbeau EJ, Towe BC, Muehlbauer MJ (1987b) A potentially implantable thermoelectric sensor for measurement of glucose. ASAIO J 33:329–335

Haque A-MJ, Park H, Sung D, Jon S, Choi S-Y, Kim K (2012) An electrochemically reduced graphene oxide-based electrochemical immunosensing platform for ultrasensitive antigen detection. Anal Chem 84:1871–1878

Heyries KA, Loughran MG, Hoffmann D, Homsy A, Blum LJ, Marquette CA (2008) Microfluidic biochip for chemiluminescent detection of allergen-specific antibodies. Biosens Bioelectron 23:1812–1818

Incropera FP (2011) Fundamentals of heat and mass transfer. Wiley, New York

Lee G-B, Chang C-C, Huang S-B, Yang R-J (2006) The hydrodynamic focusing effect inside rectangular microchannels. J Micromech Microeng 16:1024

Lerchner J, Wolf A, Wolf G, Baier V, Kessler E, Nietzsch M, Krügel M (2006) A new micro-fluid chip calorimeter for biochemical applications. Thermochim Acta 445:144–150

Mirasoli M, Guardigli M, Michelini E, Roda A (2014) Recent advancements in chemical luminescence-based lab-on-chip and microfluidic platforms for bioanalysis. J Pharm Biomed Anal 87:36–52

Muehlbauer MJ, Guilbeau EJ, Towe BC (1989) Model for a thermoelectric enzyme glucose sensor. Anal Chem 61:77–83

Muehlbauer MJ, Guilbeau EJ, Towe BC, Brandon TA (1990) Thermoelectric enzyme sensor for measuring blood glucose. Biosens Bioelectron 5:1–12

Nestorova GG, Kopparthy VL, Crews ND, Guilbeau EJ (2015) Thermoelectric lab-on-a-chip ELISA. Anal Methods 7:2055–2063

Pinacho DG, Sánchez-Baeza F, Pividori M-I, Marco M-P (2014) Electrochemical detection of fluoroquinolone antibiotics in milk using a magneto immunosensor. Sensors 14:15965–15980

Posthuma-Trumpie GA, Korf J, van Amerongen A (2009) Lateral flow (immuno) assay: its strengths, weaknesses, opportunities and threats. A literature survey. Anal Bioanal Chem 393:569–582

Ricci F, Adornetto G, Palleschi G (2012) A review of experimental aspects of electrochemical immunosensors. Electrochim Acta 84:74–83

Tangutooru SM, Kopparthy VL, Nestorova GG, Guilbeau EJ (2012) Dynamic thermoelectric glucose sensing with layer-by-layer glucose oxidase immobilization. Sens Actuators B Chem 166:637–641

Tran H, Piro B, Reisberg S, Nguyen LH, Nguyen TD, Duc H, Pham M (2014) An electrochemical ELISA-like immunosensor for miRNAs detection based on screen-printed gold electrodes modified with reduced graphene oxide and carbon nanotubes. Biosens Bioelectron 62:25–30

Wang L, Lin Q (2005) Theory and experiments of MEMS thermal biosensors. In: Engineering in medicine and biology society, 27th annual international conference of the IEEE, pp 1301–1304

Wiseman ME, Frank CW (2012) Antibody adsorption and orientation on hydrophobic surfaces. Langmuir 28:1765–1774

Wu LL, Chiou C-C, Chang P-Y, Wu JT (2004) Urinary 8-OHdG: a marker of oxidative stress to DNA and a risk factor for cancer, atherosclerosis and diabetics. Clin Chim Acta 339:1–9

Xie B, Danielsson B (1996) An integrated thermal biosensor array for multianalyte determination demonstrated with glucose, urea and penicillin. Anal Lett 29:1921–1932

Yiqun D, Wuming Z, Jiliang L, Yuquan C (1995) Mathematical model and heat conduction analysis of a silicon-based thermoelectric enzyme sensor. In: Microelectronics and VLSI, IEEE Region 10 international conference on IEEE, pp 367–370

Zhang Y, Tadigadapa S (2004) Calorimetric biosensors with integrated microfluidic channels. Biosens Bioelectron 19:1733–1743

Zhou F, Wang M, Yuan L, Cheng Z, Wu Z, Chen H (2012) Sensitive sandwich ELISA based on a gold nanoparticle layer for cancer detection. The Analyst 137:1779–1784